Linear optical properties of a high-finesse cavity dispersively coupled to a micromechanical membrane

J. G. E. Harris*[a,b], A. M. Jayich[a], B. M. Zwickl[a], C. Yang[a], J. C. Sankey[a]
[a]Department of Physics, Yale University, New Haven, CT, 06520, USA;
[a]Department of Applied Physics, Yale University, New Haven, CT, 06520, USA

ABSTRACT

We present measurements of an optomechanical system in which the mechanical element is inside the cavity, and couples dispersively to the intracavity field. This geometry makes it easier to simultaneously achieve high optical finesse and high mechanical quality factor in an optomechanical device. We measured the linear optical properties of a such a device in which the mechanical element is a 50 nm thick silicon nitride membrane. We find that the device's finesse, resonant transmission and resonant reflection can be explained with a simple model which allows us to extract the membrane's optical loss. Our results indicate that it should be possible to increase the finesse of these devices to 5×10^5 or higher.

Keywords: Radiation pressure, optomechanics, dispersive coupling, cavity QED

1. INTRODUCTION

Radiation pressure provides a unitary coupling between the electromagnetic field and the translational degrees of freedom of macroscopic objects. Optomechanical devices in which a mechanical oscillator detunes an electromagnetic cavity are the focus of research for detector applications in astrophysics, cosmology, quantum optics, and nanoscience. In addition, there is considerable interest in these devices in their own right. For example, it has been predicted that if the coupling between the optical and mechanical degrees of freedom is sufficiently strong, a number of interesting quantum effects should become manifest.[1]

Many of the optomechanical devices studied to date consist of an optical cavity in which one of the mirrors is suspended on a pliable element such as a pendulum or a micromechanical cantilever (as illustrated in Figure 1a). When this element deflects by an amount x, the cavity experiences a detuning Δ which is proportional to x. Equivalently, light stored in the cavity exerts a force (radiation pressure) on the mechanical element proportional to the intracavity power and independent of x.

To reach the quantum regime of these devices one typically wants to maximize the force per photon exerted by the cavity field on the mechanical element, as well as the element's response to this force. At the same time, it is advantageous to decrease the influence of the thermal bath. As a result, one typically wants to maximize the cavity finesse F and the mechanical element's quality factor Q, while minimizing the bath temperature T, the mechanical element's mass m and its resonant frequency ω_m.

Simultaneously achieving these goals has proved challenging, as many of the properties of high F mirrors are ill-suited to integration into sensitive mechanical devices. For example, high-F mirrors are typically formed from layers of SiO_2 and Ta_2O_5. These materials have high internal friction,[2] thereby limiting Q. They are also typically strained, so maintaining the mirror flatness requires a stiff substrate, tending to increase ω_m. Lastly, they must be large enough to avoid optical losses from diffraction (setting a minimum mirror radius[3] of ~ 20 μm) and transmission (setting a minimum mirror thickness[4] of ~ 2μm), thereby setting a lower limit on m.

A number of groups have developed fabrication techniques and/or device designs which partially resolve these apparent conflicts. However they usually involve some degree of compromise between ideal optical properties and ideal mechanical properties.

* jack.harris@yale.edu; phone 1-203-432-3826; fax 1-203-432-6275

Laser Refrigeration of Solids, edited by Richard I. Epstein, Mansoor Sheik-Bahae,
Proc. of SPIE Vol. 6907, 69070E, (2008) · 0277-786X/08/$18 · doi: 10.1117/12.760993

An alternate approach is illustrated in Figure 1b. Here the optical cavity is formed from two macroscopic rigid mirrors which are assumed to be fixed. The mechanical degree of freedom is a partially transparent dielectric slab indicated in orange. In such a system, the cavity detuning will depend on the position x of the membrane, but in a manner quite different from the systems described above. The detuning will depend upon the position of the membrane relative to the nodes and antinodes of the cavity, and so will be a periodic function of x.[5] This is an example of a dispersive coupling to a cavity field, and is reminiscent of the case of a far-off-resonant atom in a cavity. Figure 2 shows a calculation[5] of the cavity detuning as a function of x for different values of the dielectric slab's reflectivity r. Note that the strength of the optomechanical coupling (e.g. the radiation pressure) is proportional to the slope of this curve, and, for optimal x, is proportional to r.

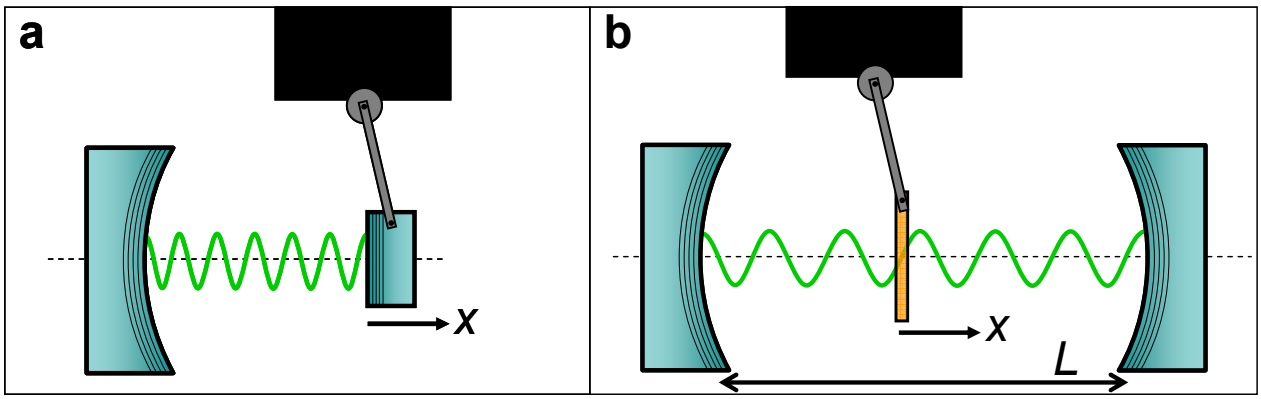

Fig. 1. Illustration of two possible geometries for optomechanical devices. In **a**, the more common "reflective" type of optomechanical coupling is shown. The movable mirror defines the right-hand boundary of the cavity, and its mechanical pliability is indicated schematically as a pendulum. The intracavity mode is shown in green. x is the mirror displacement. In **b**, the cavity mirrors are assumed to be fixed, and the mechanical degree of freedom is a dielectric slab suspended in the cavity. The total cavity length is L.

The dispersive optomechanical device described above has two noteworthy features. The first is essentially technical: in this device, the optical and mechanical functionality are segregated into physically distinct devices. The high-reflectivity end mirrors provide the cavity finesse, while the dielectric slab provides the mechanical pliability. As a result it is not necessary to integrate a high-finesse mirror into a micromechanical device. This removes many of the conflicts listed above: cavity finesse and mechanical sensitivity can be optimized separately from each other. One constraint which still applies to such a dispersive optomechanical device is that the transverse size of the cavity mode be smaller than the dielectric slab (since the slab is intended to be partially transmitting, the constraint on its thickness is relaxed).

The second noteworthy feature of this type of device is more fundamental. From the plots in Figure 2, it is clear that for certain value of x, the cavity detuning is quadratic in x: $\Delta \propto x^2$. Such a situation arises whenever the slab is positioned at a node or antinode of the cavity mode.[5] In contrast, a traditional optomechanical device (in which the mechanical element is a cavity end mirror) always has a detuning linear in x. The utility of having $\Delta \propto x^2$ arises from the fact that it means that light reflected from the cavity carries away no information about x, but only x^2. This is especially important for measurements where quantum back action is relevant, as the information extracted from the system determines the nature of the back action. It has been pointed out that "displacement-squared" measurements allow (in principle) for quantum non-demolition measurements of the energy of a mechanical oscillator.[6]

Realizing such a measurement and using it to observe quantum jumps of a macroscopic mechanical oscillator would represent a major advance in the field of quantum measurement. However the lack of a practical displacement-squared readout (as well as other experimental challenges) has precluded such a measurement.

In a recent paper[5] we described the realization of a dispersive optomechanical system in which a commercial silicon nitride membrane served as the dielectric slab and commercial mirrors mounted on an Invar spacer served as the cavity. The observed optomechanical coupling agreed well with the calculated form shown in Figure 2. Furthermore, the technical advantages associated with having distinct optical and mechanical components allowed the device to simultaneously achieve a high finesse and high-quality mechanical properties. This was exploited to laser-cool the membrane's Brownian motion from room temperature to ~ 7 mK. Lastly, a brief theoretical analysis of the feasibility of using the displacement-squared readout to observe quantum jumps of a mechanical oscillator was presented. Reference 5 represented the first measurements on this device and did not include a full characterization of the dispersive optomechanical system. A more complete study of the mechanical properties of the membranes has since been completed.[7]

Here we present measurements of the linear optical properties of this system. We focus on the dependence of the cavity finesse, resonant transmission and resonant reflection as function of membrane position. For these measurements, the mechanical properties of the membrane are irrelevant; we are merely performing linear spectroscopy on a cavity containing a fixed dielectric slab. However this is a crucial step towards having a full understanding of this device. We find that our results can be reproduced by a simple model whose only adjustable parameters are the reflectivities of the cavity end mirrors and the real and imaginary components of the membrane's index of refraction. We find that the latter agree well with previous measurements of similar systems and give an indication of how much further such a device can be improved, given present-day technology.

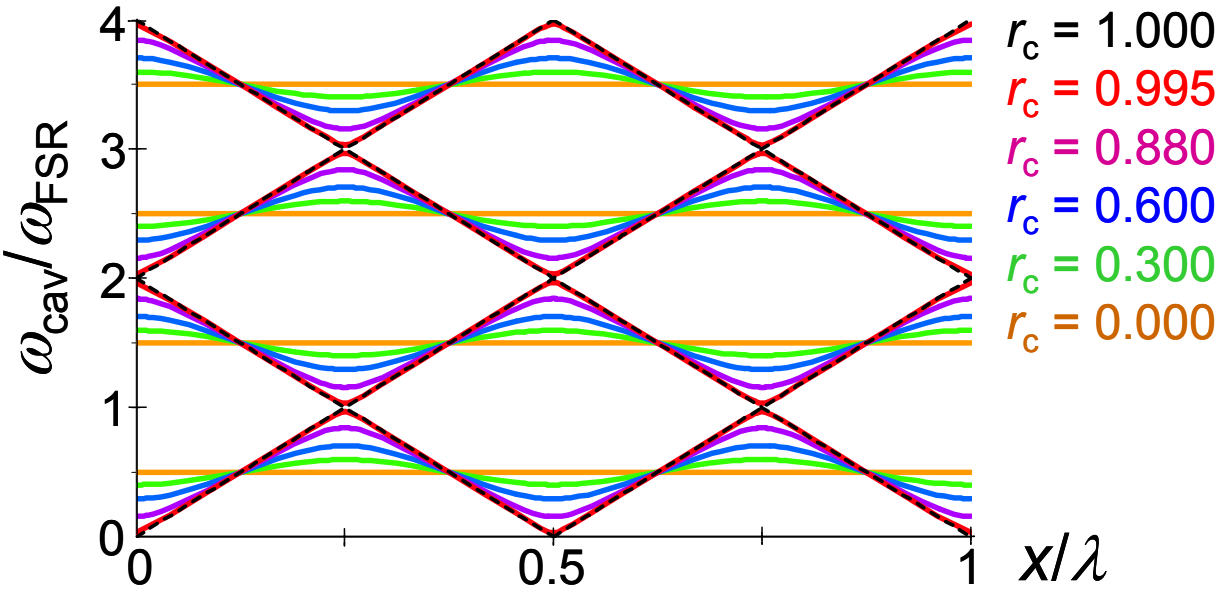

Fig. 2. A plot of the cavity resonance frequency $\omega_{cav}/\omega_{FSR}$ as a function of the membrane displacement x (ω_{FSR} is the free spectral range of the cavity). Each color corresponds to a different reflectivity of the membrane, given in the key on the right. The radiation pressure exerted by the intracavity mode on the membrane is proportional to the slope of this curve. It can be seen to change sign, corresponding to a cavity eigenmode primarily localized in one half of the cavity or the other. Note that the maximum radiation pressure for a given membrane reflectivity is proportional to the reflectivity.

2. EXPERIMENTAL

The device studied here is essentially identical to the one described in Ref. 5. An optical cavity is formed between two commercial mirrors[8] specified to give a finesse of $F = 20{,}000$. These mirrors are rigidly mounted to a spacer of length $L = 6.7$ cm machined from Invar. The spacer has a hole drilled along the cavity axis to accommodate the cavity mode, as well as a second hole perpendicular to the cavity axis which allows access to the waist of the cavity mode. Through this second hole we introduce the SiN membrane[9] into the cavity waist. The membrane's coarse position in the transverse plane of the cavity is set *ex situ* by hand. The membrane is mounted on a piezoelectric element (PZT) which can translate it *in situ* along the cavity axis by ~ 2 μm. In addition, a motorized tilt stage[10] allows the angular alignment between the membrane and the cavity mode to be adjusted *in situ*. For the measurements described here, the angular alignment was adjusted to achieve maximum transmission of the TEM_{00} mode; presumably this corresponds to the cavity axis being normal to the membrane. The cavity is mounted on passive vibration isolation pads inside a vacuum chamber which is pumped to ~ 10^{-6} Torr by an ion pump.

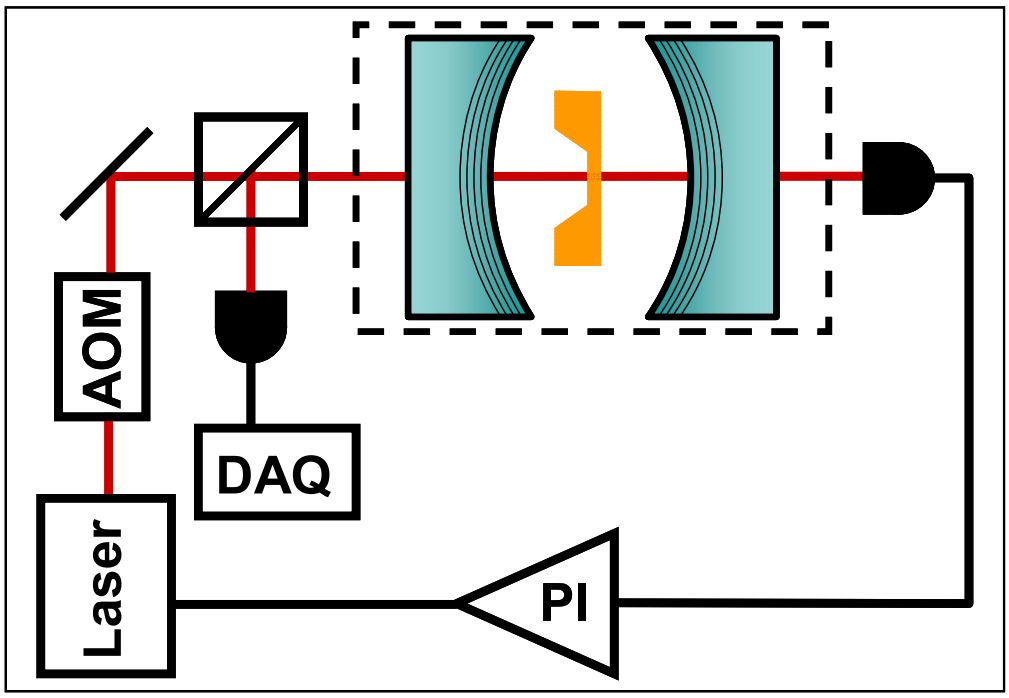

Fig. 3. Schematic of the experimental setup. Laser light from a cw Nd:YAG laser passes through an acoustooptic modulator (AOM) and input optics to illuminate the cavity. Photodiodes monitor the transmitted and reflected light. The proportional-integral (PI) feedback loop can be used to lock the cavity to the transmission signal, but is not used for the measurements described here. The cavity mirrors (blue) and membrane (orange) are mounted in vacuum (indicated by the dashed line), maintained at ~ 10^{-6} Torr by an ion pump.

The cavity is excited by a continuous-wave Nd:YAG laser[11] with wavelength $\lambda = 1064$ nm. The beampath (Figure 3) includes an optical isolator, an acoustooptic modulator (used primarily for switching off the beam for cavity ringdown measurements), and mode-matching optics for coupling the light into the cavity. Photodiodes monitor the light reflected from and transmitted through the cavity.

The membrane is a 50 nm thick SiN film suspended over a window etched into a 200 μm thick Si chip. The device is manufactured for use as a window for X-ray spectroscopy, and as a result is extremely flat, smooth, and homogenous. A photograph of a typical device is shown in Figure 4.

Figure 5 shows a measurement of the optical power transmitted through the cavity as a function of the laser frequency and the membrane position. The two distinct bands correspond to two different TEM_{00} modes (i.e., with longitudinal eigennumber differing by unity). The less-distinct bands indicated by arrows are the TEM_{20}, TEM_{11}, and TEM_{02} modes, which form a nearly degenerate triplet. The transverse modes are identified by replacing the transmission photodiode with a video camera.

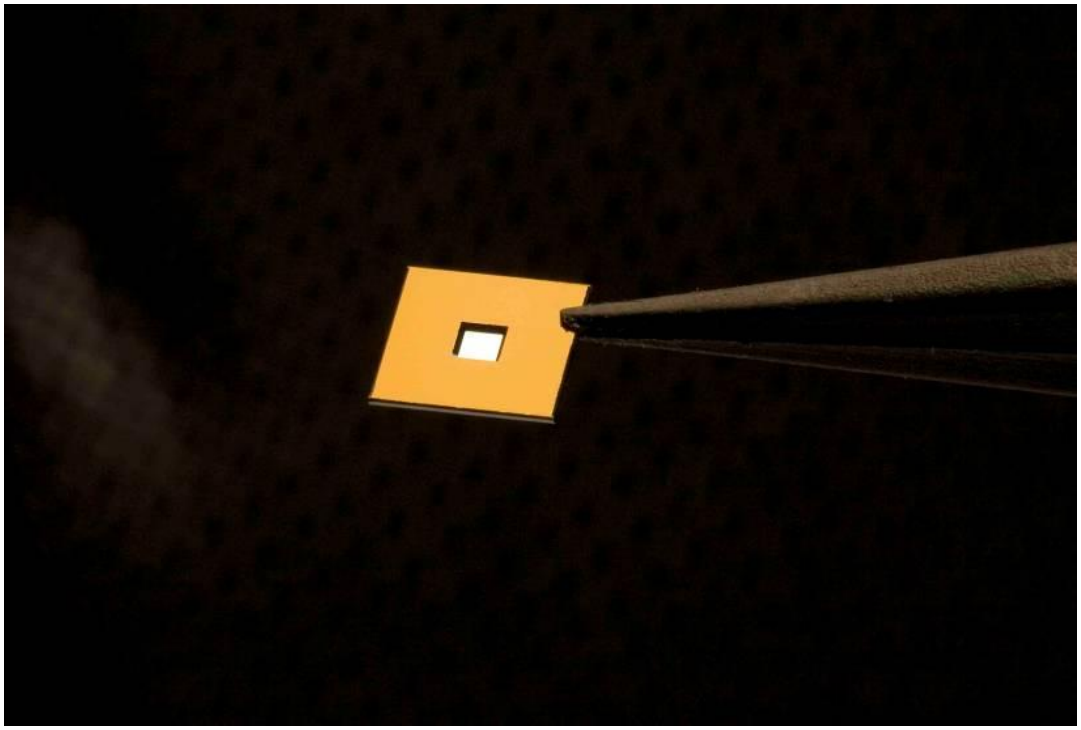

Fig. 4. Photograph of a membrane chip similar to the one used in these measurements. The orange region is the 200 μm thick Si frame from which the 50 nm thick SiN membrane (white) is suspended. The chip in the photo is held by a pair of carbon fiber tweezers.

Figures 6a and 6b show the peak value of the transmitted intensity and the minimum value of the reflected intensity for a single TEM_{00} mode as a function of the membrane position. Figure 6a essentially plots the "height" of one of the distinct bands shown in Figure 5, while Figure 6b plots the "depth" of the corresponding feature in the reflected power, both as a function of the membrane position.

Figure 6c shows the cavity finesse as a function of the membrane position. The finesse was determined by measuring the ringdown time of the intracavity field for different positions of the membrane. Figure 7 shows typical ringdown measurements for the membrane at two different positions, as well as for the membrane removed from the cavity. For these measurements the input laser was swept until the cavity transmission reached a predetermined value at which point the laser was switched off using the AOM in Figure 3. The transmitted power was observed to decay with a single exponential form regardless of the membrane position. The ringdown time was extracted from these measurements (as shown in Figure 7).

3. ANALYSIS

To model our system, we consider electromagnetic plane waves in five regions: the cavity input, the left-hand half of the cavity, the dielectric slab, the right-hand half of the cavity, and the cavity output, as indicated in Figure 8. The boundary

conditions between each region are set by either the end mirror's reflectivity and loss (which we take as fitting parameters) or the dielectric slab's index of refraction n which we take to be a complex-valued fitting parameter.

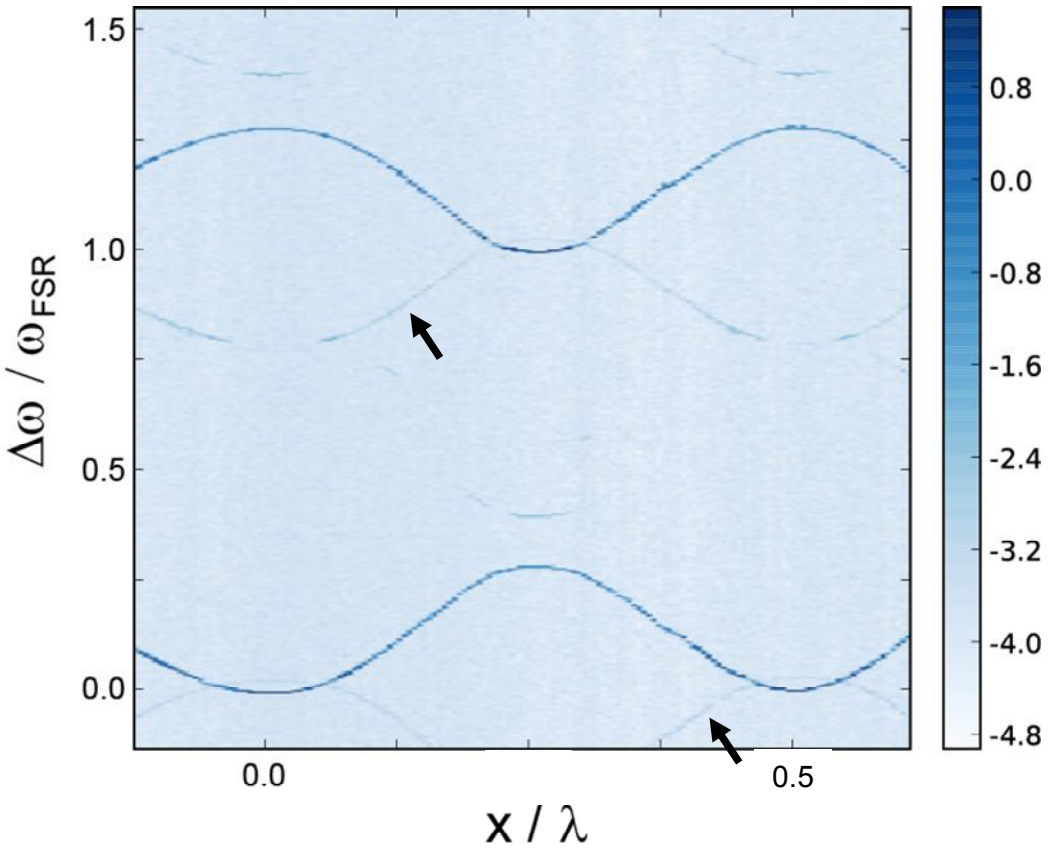

Fig. 5. Spectroscopy of the optomechanical cavity. The transmission through the cavity is plotted in color scale as a function of the laser detuning (vertical axis) and membrane position (horizontal axis). The two most distinct bands are TEM_{00} cavity modes, while the bands indicated by arrows are the TEM modes whose indices sum to 2.

Assuming light is incident only from the input side (as is the case in the experiment), we solve the resulting set of coupled equations and find the transmitted and reflected power as a function of the incident laser frequency and the membrane position. This allows direct comparison with the data in Figures 6a and 6b. To compare the measured finesse (Figure 6c) with our model, we determine the theoretical $F(x)$ curve by plotting the calculated transmission as a function of the laser detuning for a given x and finding its linewidth numerically.

The fits resulting from this procedure are shown as solid lines in Figures 6a, 6b, and 6c. They are all periodic in x with the period of the intracavity standing wave: $\lambda/2$. The $F(x)$ curve is particularly noteworthy because it has the most intuitive connection to the fitting parameters. The maximum of this curve, ~ 16,000, is very close to the finesse measured for the empty cavity, while the minimum (~ 6,500) is considerably lower. This can be understood as resulting from the fact that the membrane is much thinner than λ, so when it is placed at a node of the cavity mode it sees only a very weak intracavity field. As a result the rate at which photons are absorbed or scattered from the intracavity field is much smaller than if the same membrane was exposed to a traveling beam of the same intensity. A similar suppression of losses is exploited in blue-detuned optical lattices, in which atoms are trapped at nodes of the optical field and so have a greatly reduced rate of scattering.[12]

When the membrane is moved away from a node, the optical losses increase until they reach a maximum (i.e., a minimum in $F(x)$) when the membrane is at an antinode of the cavity mode.

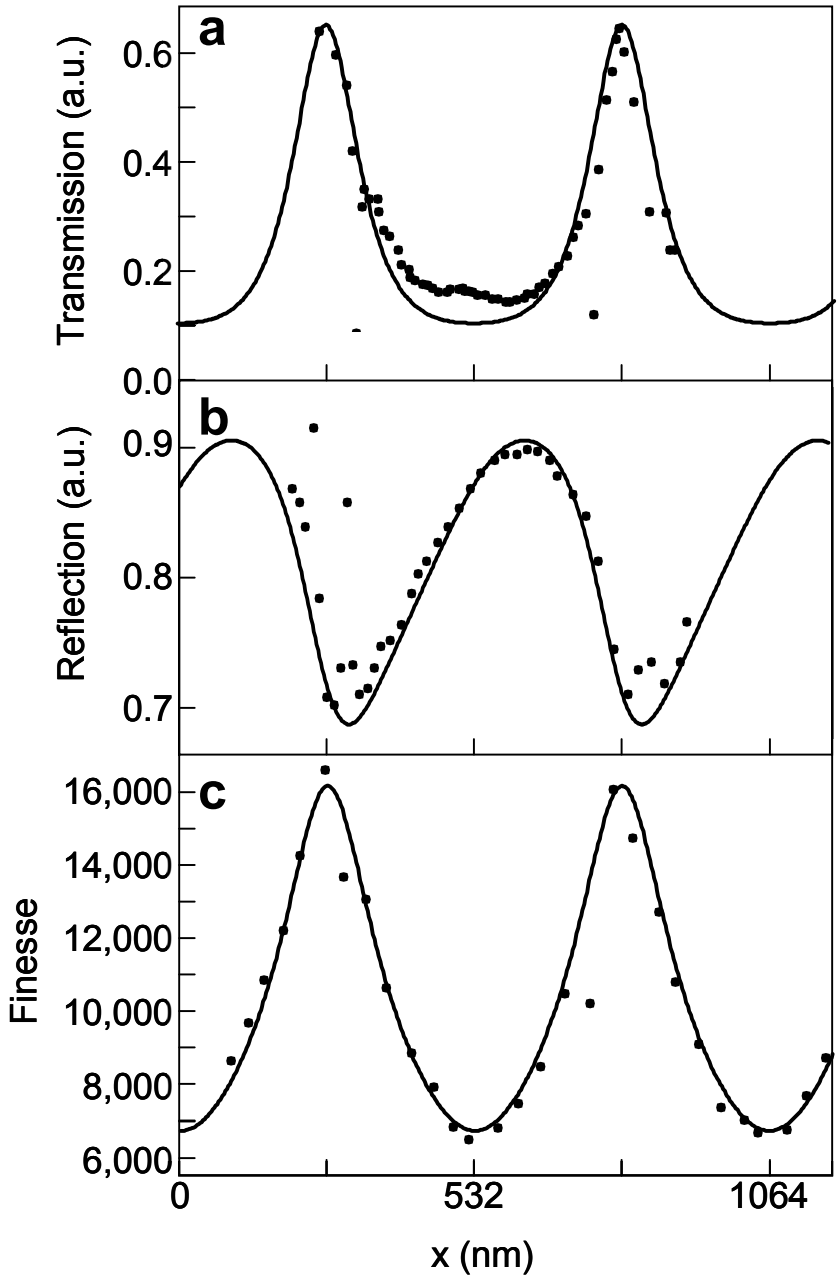

Fig. 6. Optical properties of the optomechanical system. **a** shows the maximum (i.e., peak) transmission on resonance for a TEM_{00} mode is shown as a function of membrane position. The corresponding minimum in the reflection is shown in **b**. The data in both **a** and **b** were extracted from scans similar to the one in Figure 5. The cavity finesse as a function of membrane position is shown in **c**. The cavity finesse was determined from ringdown measurements similar to the ones shown in Figure 7. The fits are described in the text.

The values extracted from the fits shown in Figures 6a, 6b, and 6c are: $F_0 = 16{,}500$ (this is the finesse of the end mirrors, which we assume are symmetric), and $n = 2.2 + 1.5 \times 10^{-4}\, i$. This value for F_0 agrees well with the empty-cavity ringdown measurement (Figure 7) as well as the manufacturer's specification. The real part of n also agrees with tabulated values. The imaginary part of n, which is responsible for lowering the cavity finesse below F_0 when the membrane is not at a node, has not been measured for comparable thin films of SiN at 1064 nm. However, extrapolating the data in Reference 13 (taken at slightly shorter wavelengths) agrees fairly well with our measured value.

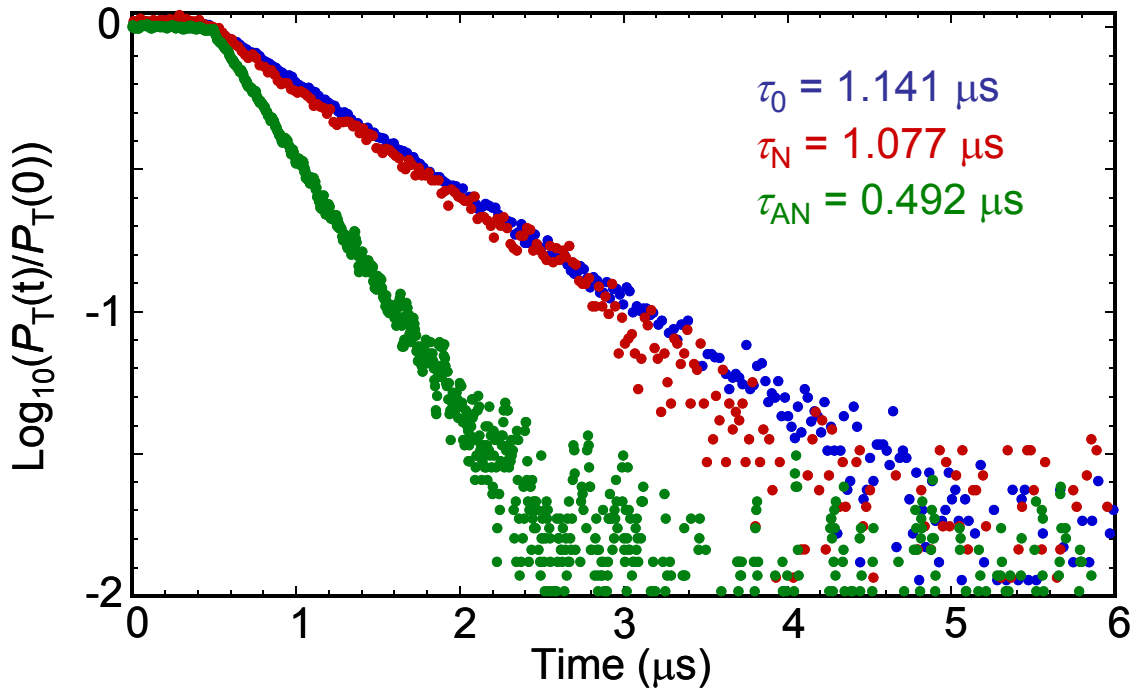

Fig. 7. Cavity ringdown measurements used to determine the finesse. The blue data shows a ringdown measurement for the empty cavity, while the red and green data correspond to the membrane at a node or antinode, respectively, of the cavity mode. The time constant for each ringdown measurement is given in the figure.

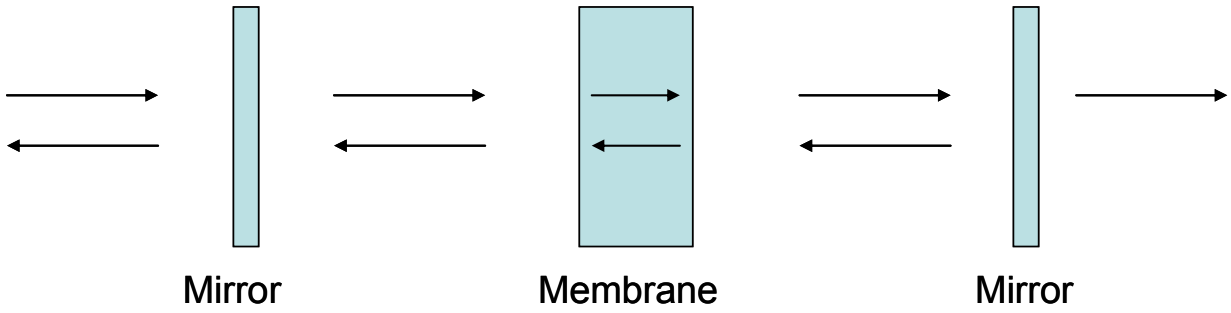

Fig. 8. Illustration of the model used to calculate the curves in figure 6. Each arrow corresponds to a plane electromagnetic wave. The laser light is incident from the left.

4. DISCUSSION

The data and fits in Figures 6a, 6b, and 6c indicate that linear optical properties of this device are well-described by the simple model outlined above. The agreement between the fitting parameters and the expected values of the end mirrors' reflectivity and the membrane's n also attest to our understanding of this system. In order to exploit this understanding and push these devices closer to their quantum regime, we would like to know how much further the cavity finesse can be increased. The ultimate limit will be set by the maximum reflectivity of commercially available mirrors (which to date[14] have achieved $F > 10^6$) and the intracavity loss induced by the membrane (which is set by the imaginary part of n).

To answer this question we have calculated the $F(x)$ curves for various values of the end mirror refelctivities (parameterized by the empty cavity finesse F_0 they would produce) assuming that n is given by the value extracted from the fits in Figure 6. As with the fit in Figure 6c, the calculation proceeds by calculating the transmission curve as a function of x and determining the resonance linewidths numerically. The results are shown in Figure 9 for F_0 = 105,000; 314,000; 1,050,000. Although the loss in the membrane keeps F low when the membrane is at an antinode (i.e., the minima in the curves of Figure 9), the advantage of placing the membrane at a node is seen quite clearly. For an empty cavity finesse of 105,000, the membrane only lowers the finesse by ~ 10%. For state-of-the-art end mirrors, the finesse still exceeds 500,000.

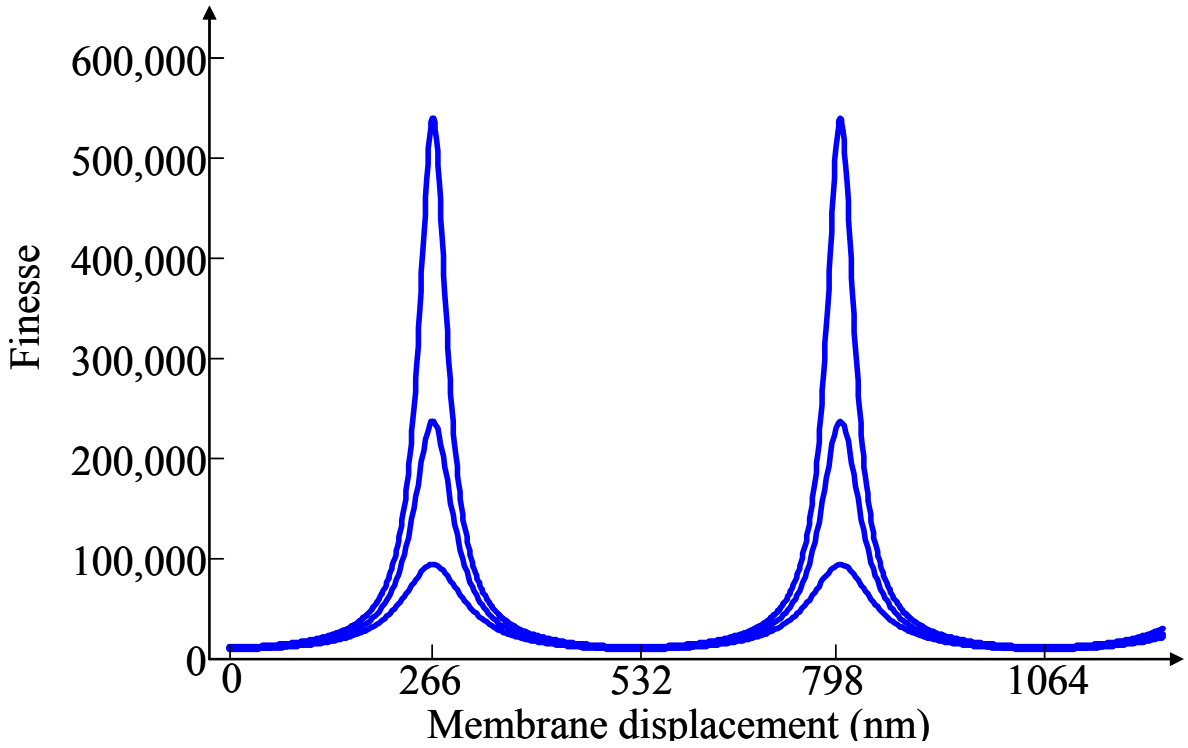

Fig. 9. The calculated finesse as a function of membrane position assuming a membrane whose complex index of refraction is the same as that determined from the fits in Figure 6. The curves, from bottom to top, correspond to end mirrors with finesse of 105,000, 314,000, and 1,050,000.

Although many applications require operating the optomechanical system with the membrane off a node, we note that the goal of reading out the energy eigenstate of the membrane (as described in Reference 5) explicitly requires that the membrane be at a node (or antinode). Thus the results in Figure 9 indicate that the finesse assumed in the calculations in

Reference 5 can be achieved using present-day mirror technology and the SiN membranes already in our lab. If higher finesse is required (or operation away from a node), it may be advantageous to work at longer wavelengths, as the absorption of SiN seems to trend downward with increasing λ.[13]

ACKNOWLEDGEMENTS

We gratefully acknowledge discussions with Florian Marquardt and Steven Girvin, and the photography of Bernie Staggers. This work was supported by the NSF (grants #0555824 & 0653377). J. G. E. H. acknowledges support from a Sloan Research Fellowship. B. M. X. Acknowledges an NSF Graduate Research Fellowship.

REFERENCES

[1] C. Fabre *et al*. Phys. Rev. A **49**, 1337 (1994); V. Giovannetti *et al.*, Europhysics Lett. **54**, (2001); D. Vitali, Phys. Rev. Lett. **98**, 030405 (2007); M. Pinard *et al.*, Europhys. Lett. **72**, 747 (2005); S. Bose *et al.*, Phys. Rev. A **59**, 3204 (1999); W. Marshall *et al.*, Phys. Rev. Lett. **91**, 130401 (2003); A. Fereira *et al.*, Phys. Rev. Lett. **96**, 060407 (2006).
[2] G. M. Harry *et al*., Class. Quantum Grav. **19**, 897 (2002).
[3] D. Kleckner *et al*., Phys. Rev. Lett. **96**, 173901 (2006).
[4] C. J. Hood *et al.,* Phys. Rev. A **64**, 033804 (1999).
[5] J. D. Thompson *et al.*, arXiv:0707.1724 (2007).
[6] V. B. Braginsky *et al.* Science **209**, 547 (1980); D. H. Santamore *et al*., Phys. Rev. B **70**, 144301 (2004); I. Martin and W. H. Zurek, Phys. Rev. Lett. **98**, 120401 (2007).
[7] B. M. Zwickl *et al*., arXiv:0711.2263 (2007).
[8] Advanced Thin Films, Longmont, CO, USA..
[9] Norcada Inc., Edmonton AB, Canada.
[10] Thorlabs Inc., Newton, NJ, USA.
[11] Innolight GmbH, Hannover, Germany.
[12] T. Müller-Seydlitz *et al*., Phys. Rev. Lett. **78**, 1038 (1997).
[13] D. P. Poenar and R. F. Wolffenbuttel, *Appl. Opt.* **36**, 5122 (1997).
[14] G. Rempe *et al*., Optics Letters **17**, 363 (1992).